Confidence in Detection and Discrimination: an fMRI Study

Matan Mazor, Karl J. Friston and Stephen M. Fleming

Objective

The current study aims to compare the brain processes that govern perceptual discrimination and detection, and the neural mechanisms that allow for metacognitive evaluations of these processes.

A fundamental property that distinguishes detection from discrimination tasks is the asymmetry in the availability of evidence for 'yes' and for 'no' responses. While discrimination requires a comparison between the relative evidence for different options, in a detection setting evidence can only be available for the presence of a stimulus and not for its absence. Conceptually, this means that confidence in the absence of a stimulus cannot rely on the magnitude of evidence for its absence and may rely instead on counterfactual reasoning regarding the likelihood of the stimulus to be detected had it been presented. Behaviorally, this difference is reflected in general lower confidence and in a weaker association between objective accuracy and subjective confidence for 'no' responses (Kanai, Walsh, & Tseng, 2010; Meuwese, van Loon, Lamme, & Fahrenfort, 2014) in detection but also in detection-like tasks (such as recognition memory; Higham, Perfect, & Bruno, 2009).

It is still unknown what are the brain mechanisms that give rise to these behavioral differences. In previous studies comparing structural and functional correlates of metacognitive sensitivity ratings across domains (Mccurdy, Maniscalco, Metcalfe, & De Lange, 2013; Morales, Lau, & Fleming, 2018), care was taken to equate task requirements

and avoid the asymmetry inherent to true detection tasks. For example, instead of asking participants to perform 'old'/'new' recognition judgments, participants were asked to answer which of two presented stimuli is old. Similarly, instead of asking participants whether they detected a signal or not, a 2 Interval Forced Choice (2IFC) approach is often preferred, where participants are asked to report whether the signal was presented in the first or the second interval.

Here we wish to compare detection and discrimination within the same low-level perceptual task, while controlling for differences in task performance. The objectives of this study are:

1. Replicate previous findings of a generic confidence signal in the activity of medial prefrontal cortex (De Martino, Fleming, Garrett, & Dolan, 2013; Morales et al., 2018).
2. Test for an interaction between confidence level and task (detection/discrimination) in the BOLD response, specifically in the prefrontal cortex.
3. Within detection, test for an interaction between confidence level and response (yes/no) in the BOLD response, specifically in the prefrontal cortex and in regions that have previously been associated with counterfactual reasoning (Boorman, Behrens, & Rushworth, 2011; Neubert, Mars, Thomas, Sallet, & Rushworth, 2014).
4. Test for relationships between fluctuations in metacognitive adequacy (a trial-by-trial measure of metacognitive sensitivity; Wokke, Cleeremans, & Ridderinkhof, 2016) and the BOLD signal separately for detection and for discrimination, and for yes and no responses within detection.

5. Replicate previous findings of inter-subject correlations of functional properties of the lateral prefrontal cortex (lPFC) with metacognitive efficiency (meta-d'/d'; Fleming & Lau, 2014) in discrimination (Yokoyama et al., 2010).
6. Identify inter-subject functional correlates of metacognitive efficiency in detection. Specifically, we will be interested to see if metacognitive efficiency in detection is predicted by different brain structures than metacognitive efficiency in discrimination.

Design

We will test 35 healthy subjects in a 3 Tesla MRI scanner in the Welcome Centre for Human Neuroimaging, Institute of Neurology, University College London.

Participants will be acquainted with the task in a preceding behavioural session. During this session, task difficulty will be adjusted independently for detection and for discrimination, targeting around 70 % accuracy on both tasks.

The scanning session will start with a structural MP-RAGE scan, followed by a fieldmap scan. During this time, participants will perform a staircase procedure similar to that performed in the preceding behavioural session. This calibration phase is used to further calibrate participants' performance on both tasks inside the MRI scanner. After completing the calibration phase, participants will undergo 5 ten-minute functional scanner runs, each comprising one detection and one discrimination block of 40 trials each, presented in random order.

After a temporally jittered rest period of 500-4000 milliseconds, each trial will begin with a fixation cross (500 milliseconds), followed by a presentation of a target for 33 milliseconds. In discrimination trials, the target will be a circle of diameter 3° containing randomly generated white noise, merged with a sinusoidal grating (2 cycles per degree; oriented 45° or -45°). In half of the detection trials, targets will not contain a sinusoidal grating and will

consist of random noise only. After the offset of the stimuli, participants will use their right-hand index and middle fingers to make a perceptual decision about the orientation of the grating (discrimination blocks), or about the presence or absence of a grating (detection blocks). The response mapping will be counterbalanced between blocks, such that an index finger press will be used to indicate a clockwise tilt on half of the trials, and a counterclockwise tilt on the other half. Similarly, in half of the detection trials the index finger will be mapped to a 'yes' response, and on the other half to a 'no' response. Participants will then use their left-hand thumb to rate their confidence in their decision on a 6-point scale. The perceptual decision and the confidence rating phases will be restricted to 1500 and 2500 milliseconds, respectively. No feedback will be delivered to subjects about their performance.

To avoid stimulus-driven fluctuations in confidence, grating contrast will be fixed within each experimental block. Nevertheless, following experimental blocks with markedly bad ($\leq 52.5\%$) or good ($\geq 85\%$) accuracy, grating contrast will be adjusted for the next block of the same task (contrast level will be divided or multiplied by a factor 0.9 for bad and good performance, accordingly). Finally, grating contrast will be adjusted for both tasks following runs in which the difference in performance between the two tasks exceeded 16.25% (contrast level will be multiplied by the square root of 0.9 for the easier task and divided by the square root of 0.9 for the more difficult task).

Confidence rating

Subjects will rate their confidence on a 6-point scale by using two keys to increase and decrease their reported confidence level with their left-hand thumb. Confidence levels will be indicated by the size and color of a circle presented at the center of the screen. The initial size and color of the circle will be determined randomly at the beginning of the confidence rating phase, to make the number of button presses independent from the final confidence

rating. The mapping between color and size to confidence will be counterbalanced between participants: for half of the participants, high confidence will be mapped to small, red circles, and for the other half, high confidence will be mapped to large, blue circles. This counterbalancing is employed to isolate confidence-related activations from activations that originate from the perceptual properties of the confidence scale or from differences in the motor requirement to press the upper and lower buttons.

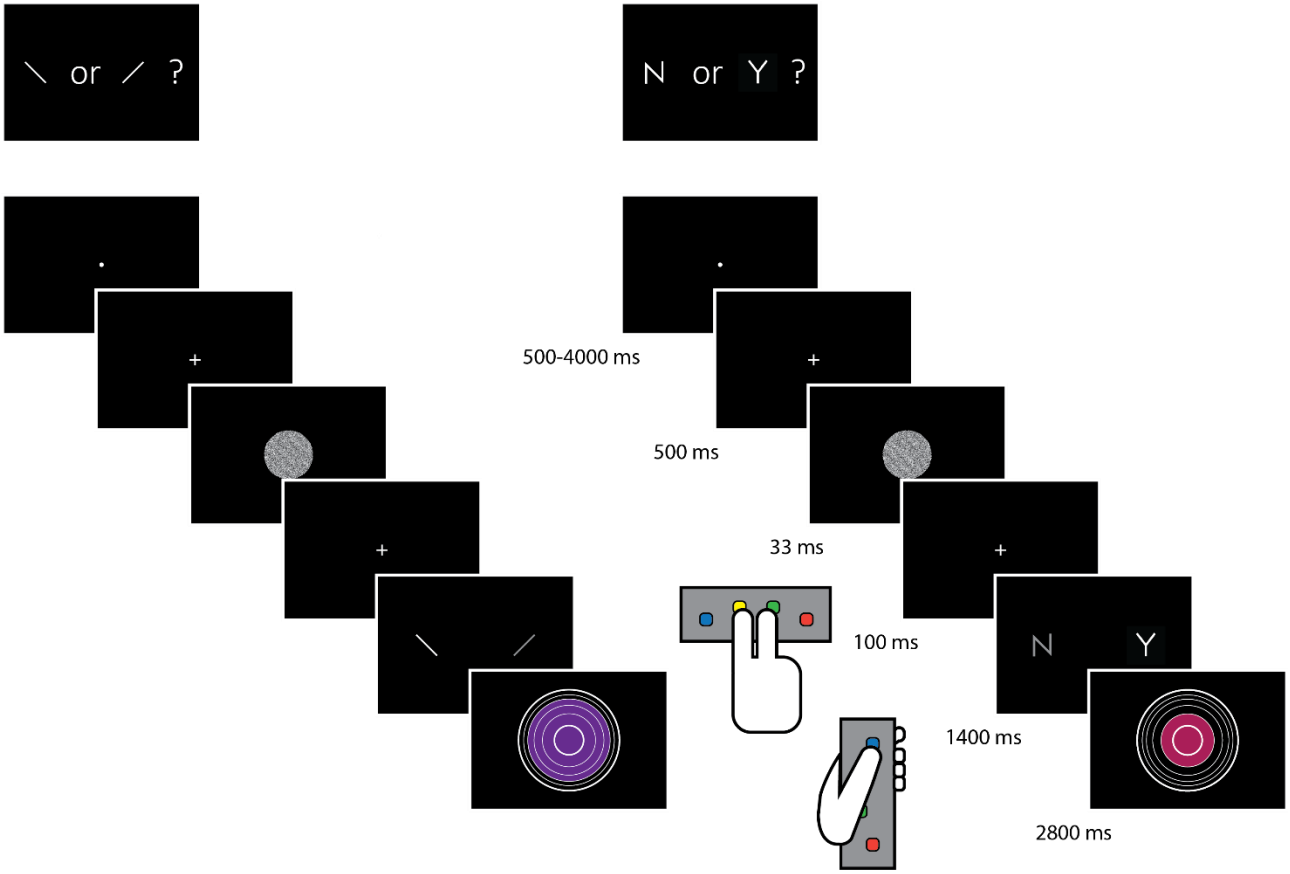

Figure 1: Experimental design for discrimination and for detection trials. Perceptual decisions are reported using the right index and middle fingers, and confidence ratings are reported using the left thumb. Confidence rating will be made by varying the size and color of a circle, with 6 options ranging from small and red to big and blue. For half of the subjects, high confidence will be mapped to the small, red circle. For the other half, high confidence will be mapped to the big, blue circle. The initial size and color of the circle will be determined randomly at the beginning of the confidence rating phase, to make the number of button presses independent from the final confidence rating.

Bonus

To incentivize participants to do their best at the task and rate their confidence accurately, a bonus payment will be offered:

$$bonus = \overrightarrow{accuracy} \cdot \overrightarrow{confidence}$$

Where $\overrightarrow{accuracy}$ is a vector of 1 and -1 for correct and incorrect responses, and $\overrightarrow{confidence}$ is a vector of integers in the range of 1 to 6, representing confidence reports for all trials. The payment structure will be explained to participants in the preceding behavioural session. Specifically, participants will be advised that to maximize their bonus they should do their best at the main task, rate the confidence higher when they believe they are correct, and rate their confidence lower when they believe they might be wrong.

Scanning Parameters

Scanning will take place at the Wellcome Centre for Human Neuroimaging, London. We will use a Siemens Prisma MRI scanner with a 64-channel head coil.

We will acquire structural images using an MPRAGE sequence (1x1x1mm voxels, 176 slices, in plane FoV = 256x256 mm^2), followed by a double-echo FLASH (gradient echo) sequence with TE1=10ms and TE2=12.46ms (64 slices, slice thickness = 2mm, gap = 1mm, in plane FoV= 192×192 mm^2, resolution = 3×3 mm^2) that will later be used for field inhomogeneity correction.

Functional scans will be acquired using a 2D EPI sequence, optimized for regions near the orbito-frontal cortex (3.0x3.0x3.0mm voxels, TR=3.36 seconds, TE = 30 ms, 48 slices tilted by -30 degrees with respect to the T>C axis, matrix size = 64x72, Z-shim=-1.4).

Analysis

Behavioural Analysis

1. We will perform a t-test to compare accuracy levels between the two tasks across subjects.
2. Using a t-test on the subject-wise response probabilities ((p(response='yes') and p(response='CW')) we will test for consistent response bias effects across participants.

3. We will compare metacognitive sensitivity and bias between detection and discrimination tasks
4. Based on previous work and pilot data, we predict lower metacognitive sensitivity for 'no' than for 'yes' responses in the detection task. To quantify this effect, we will plot the response-conditional type 2 Receiver Operator Characteristic (ROC) curves within the detection task, and compare the areas under the curves for the different responses (Meuwese et al., 2014).

fMRI data preprocessing

Data preprocessing will follow the procedure described in Morales and colleagues (2018):

> *Imaging analysis will be performed using SPM12 (Statistical Parametric Mapping; www.fil.ion.ucl.ac.uk/spm). The first five volumes of each run will be discarded to allow for T1 stabilization. Functional images will be realigned and unwarped using local field maps (Andersson et al., 2001) and then slice-time corrected (Sladky et al., 2011). Each participant's structural image will be segmented into gray matter, white matter, CSF, bone, soft tissue, and air/background images using a nonlinear deformation field to map it onto template tissue probability maps (Ashburner and Friston, 2005). This mapping will be applied to both structural and functional images to create normalized images to Montreal Neurological Institute (MNI) space. Normalized images will be spatially smoothed using a Gaussian kernel (6 mm FWHM). We set a within-run 4 mm affine motion cutoff criterion.*

Preprocessing and construction of first- and second-level models will use standardized pipelines and scripts available at https://github.com/metacoglab/MetaLabCore/

Exclusion Criteria

Subject exclusion

Subjects will be excluded from all analyses in the following cases:

1. They missed more than 20% of the trials.
2. Their mean accuracy in one of the tasks was lower than 60%.
3. They exceeded the head motion cutoff criterion in more than 2 experimental runs.
4. They were heavily biased toward a particular response in one of the tasks, i.e., used the same response in more than 75% of the trials.

Subjects will be excluded from any confidence-based analysis in the following cases:

5. They used the same confidence level for more than 80% of all trials.
6. For a particular response, they used the same confidence level for more than 80% of the trials.

Run exclusion

Individual experimental runs will not be analysed in the following cases:

1. More than 20% of the trials in the run were missed.
2. Mean accuracy in one of the tasks was lower than 60%.
3. There was a heavy bias toward one response in one of the tasks, i.e., the participant used the same response in more than 80% of the trials.

Experimental runs will not be used in the confidence analysis if:

1. The same confidence level was used for more than 95% of all trials.
2. For a particular response, the same confidence level was reported for more than 95% of the trials.

Regions of Interest

In addition to an exploratory whole-brain analysis (corrected for multiple comparisons at the cluster level), our analysis will focus on the following *a priori* regions of interest, largely following the ROIs used at Fleming, van der Putten, & Daw, 2018:

1. *Frontopolar cortex* (FPC, defined anatomically). We will use a connectivity-based parcellation (Neubert et al., 2014) to define a general FPC region of interest as the total area spanned by areas FPl, FPm and BA46. The right hemisphere mask will be mirrored to create a bilateral mask.
2. *Ventromedial prefrontal cortex* (vmPFC). The vmPFC ROI will be defined as a 8-mm sphere around MNI coordinates [0,46,-7], obtained from a meta-analysis of subjective-value related activations (Bartra, McGuire, & Kable, 2013) and aligned to the cortical midline.
3. *Bilateral ventral striatum.* The ventral striatum ROIs will be specified anatomically from the Oxford-Imanova Striatal Strctural Atlas included with FSL (http://fsl.fmrib.ox.ac.uk).
4. *Posterior medial frontal cortex (pMFC).* The pMFC ROI will be defined as a 8-mm sphere around MNI coordinates [0, 17, 46], obtained from a functional MRI study on decision confidence (Fleming, Huijgen, & Dolan, 2012) and aligned to the cortical midline.
5. *Precuneus.* The precuneus ROI will be defined as a 8-mm sphere around MNI coordinates [0,-57,18], based on Voxel Based Morphometry studies of metacognitive efficiency (Fleming et al., 2010; Mccurdy et al., 2013) and aligned to the cortical midline.

For the FPC ROI, a small-volume correction will be applied to individual voxels within the ROI for all univariate contrasts. For the multivariate analysis, we will use a searchlight approach to scan for spatial patterns within the ROI, followed by a correction for multiple comparisons.

For all other ROIs, a GLM model will be fitted to the mean time course of voxels within the region, and multivariate analysis will be performed on all the voxels within the ROI.

Univariate Analysis

The univariate analysis will be based on a design matrix in which different trial types are modeled by different regressors (main design matrix, below). Additionally, to examine the global effect of confidence across trial types, a simpler design matrix will be fitted to the data as a first step (global confidence design matrix, below).

Global Confidence Design Matrix

The global confidence design matrix will consist of only 4 regressors of interest. The first two primary regressors will be 'correct trials' (trials in which the participant was correct, across tasks and responses) and 'incorrect trials' (trials in which the participant was incorrect, across tasks and responses). Single events will be modeled by a boxcar regressor with nonzero entries at the 4000 millisecond interval starting at the offset of the stimulus and ending immediately after the confidence rating phase, and will be convolved with the canonical hemodynamic response function (HRF). Additionally, the design matrix will include a confidence parametric modulator for each of the first two regressors.

The construction of the regressors and the additional nuisance regressors will be handled similarly to the main design matrix (see below).

We will use the parameter estimates from this design matrix to extract a group-level map of confidence modulation in correct responses, across all tasks and conditions.

Main Design Matrix

The main design matrix for the univariate GLM analysis will consist of 16 regressors of interest. There will be a regressors for each of the eight combinations of *task x condition x response*: For example, there will be a regressor for detection trials where a signal was present ('Yes') and the subject reported seeing a signal ('Yes'; Y_Y). The relevant trials will be modeled by a boxcar regressor with nonzero entries at the 4000 millisecond interval starting

at the offset of the stimulus and ending immediately after the confidence rating phase. This regressor will then be convolved with the canonical hemodynamic response function (HRF).

Each of these primary regressors will be accompanied by a parametric modulator, indicating the reported confidence for each trial. Together, this makes a total of 16 regressors:

		Task	**Stimulus**	**Response**
1	*CW_CW*	Discrimination	Clockwise	Clockwise
2	*CW_CCW_conf*			
3	*CW_CCW*	Discrimination	Clockwise	Counterclockwise
4	*CW_CCW_conf*			
5	*CW_CW*	Discrimination	Counterclockwise	Clockwise
6	*CW_CW_conf*			
7	*CCW_CCW*	Discrimination	Counterclockwise	Counterclockwise
8	*CCW_CCW_conf*			
9	*Y_Y*	Detection	Signal	Yes
10	*Y_Y_conf*			
11	*Y_N*	Detection	Signal	No
12	*Y_N_conf*			
13	*N_Y*	Detection	Noise	Yes
14	*N_Y_conf*			
15	*N_N*	Detection	Noise	No
16	*N_N_conf*			

Blue and red cells represent correct and incorrect responses, respectively.

In addition, trials in which the participant did not respond within the 1500 millisecond time frame will be modeled by a separate regressor. The design matrix will also include a run-wise constant term regressor, an instruction-screen regressor for the beginning of each block, four motor response regressors for each of the four response buttons, motion regressors (the 6 motion parameters and their first derivatives as extracted by SPM in the head motion correction preprocessing phase) and regressors for physiological measures.

We will apply the following contrasts to the voxel-wise beta estimates:

Contrast	Interpretation
1. Task (Y_Y + Y_N + N_Y + N_N) - (CW_CW + CW_CCW + CCW_CW + CCW_CCW)	Brain regions showing a main effect of task.
2. No – Yes responses (N_N + Y_N) – (Y_Y + N_Y)	Brain regions showing an effect of response within the detection task.
3. Confidence Y_Y_conf + Y_N_conf + N_Y_conf + N_N_conf + CW_CW_conf + CW_CCW_conf + CCW_CW_conf + CCW_CCW_conf	Brain regions showing linear modulation of reported confidence on BOLD signal.
4. **Metacognitive Adequacy (confidence x accuracy interaction)** (Y_Y_conf + N_N_conf + CW_CW_conf + CCW_CCW_conf) - (Y_N_conf + N_Y_conf + CW_CCW_conf + CCW_CW_conf)	Brain regions showing different linear modulations of confidence on the BOLD signal for correct and for incorrect responses.
5. Confidence x task interaction (Y_Y_conf + Y_N_conf + N_Y_conf + N_N_conf) – (CW_CW_conf + CW_CCW_conf + CCW_CW_conf + CCW_CCW_conf)	Brain regions showing differential modulation of confidence as a function of task.
6. Metacognitive Adequacy x task interaction (confidence x accuracy x task interaction) ((Y_Y_conf + N_N_conf) - (N_Y_conf + Y_N_conf)) – ((CW_CW_conf +	Brain regions showing different linear modulations of confidence on the BOLD signal

CCW_CCW_conf)- (CW_CCW_conf + CCW_CW_conf))	for correct and for incorrect responses.
7. Confidence in 'No' – Confidence in 'Yes' (N_N_conf + Y_N_conf) – (Y_Y_conf + N_Y_conf)	Brain regions showing a differential modulation of confidence as a function of response, in the detection task.
8. Metacognitive adequacy in 'No' – metacognitive adequacy in 'Yes' (confidence x accuracy x response interaction) (N_N_conf - Y_N_conf) – (Y_Y_conf - N_Y_conf)	Brain regions showing a differential modulation of metacognitive adequacy as a function of response, in the detection task.

Results from the above-mentioned contrasts will be followed up to rule out alternative explanations when such explanations are available. For example, to exclude the possibility that confidence effects reflect only trial-by-trial response-time variability, the robustness of the results will be tested against a design matrix that controls for variability in response time.

Group level inference

Group level inference will follow an ordinary least squares (OLS) procedure on the subject-specific contrast maps. Correction for multiple comparisons will be performed at the cluster level, using a significance threshold of P=0.05 and a cluster defining threshold of P=0.001.

Between-subject correlations

Subject-specific maps of the contrast (CCW_CCW_conf + CW_CW_conf) will be correlated against metacognitive efficiency scores for discrimination. Similarly, subject-specific maps of

the contrast (Y_Y_conf+N_N_conf) will be correlated against metacognitive efficiency scores in detection. Here also the 5 a-priori ROIs will be analyzed separately.

Multivariate analysis

Multi-voxel pattern analysis (Norman, Polyn, Detre, & Haxby, 2006) will be used to test for consistent spatial patterns in the fMRI data. We will use The Decoding Toolbox (Hebart, Gargen, & Haynes, 2015) and follow the procedures described by Morales and colleagues (2018).

Train	Test	Interpretation
High confidence vs. Low confidence (within correct trials)	High confidence vs. Low confidence (within correct trials)	Spatially multivariate signal predicting confidence reports.
Within discrimination correct trials: high confidence vs. Low confidence	Within discrimination correct trials: high confidence vs. low confidence	Spatially multivariate signal predicting confidence reports in discrimination.
Within detection correct trials: high confidence vs. Low confidence	Within detection correct trials: high confidence vs. low confidence	Spatially multivariate signal predicting confidence reports in detection.
Within discrimination correct trials: high confidence vs. Low confidence	Within detection correct trials: high confidence vs. low confidence	Task invariant multivariate signal predicting confidence reports in detection and discrimination.
Within detection correct trials: high confidence vs. low confidence	Within discrimination correct trials: high confidence vs. Low confidence	
Within detection correct trials: hits vs. misses	Within detection correct trials: hits vs. misses	Spatially multivariate signal predicting response in detection signal trials.

Within detection correct trials: Hits vs. Misses	Within discrimination trials: high vs. low confidence	Task invariant spatially multivariate signal representing the availability of perceptual evidence for stimulus presence.
Within discrimination trials: high vs. low confidence	Within detection correct trials: Hits vs. Misses	

A contrast between the last two maps will highlight brain regions that are specifically involved in inference about presence and absence, rather than judgment of available evidence *per se*.

Bartra, O., McGuire, J. T., & Kable, J. W. (2013). The valuation system: A coordinate-based meta-analysis of BOLD fMRI experiments examining neural correlates of subjective value. *NeuroImage*, *76*, 412–427. https://doi.org/10.1016/j.neuroimage.2013.02.063

Boorman, E. D., Behrens, T. E., & Rushworth, M. F. (2011). Counterfactual Choice and Learning in a Neural Network Centered on Human Lateral Frontopolar Cortex. *PLoS Biology*, *9*(6), e1001093. https://doi.org/10.1371/journal.pbio.1001093

De Martino, B., Fleming, S. M., Garrett, N., & Dolan, R. J. (2013). Confidence in value-based choice. *Nature Neuroscience*, *16*(1), 105–110. https://doi.org/10.1038/nn.3279

Fleming, S. M., Huijgen, J., & Dolan, R. J. (2012). Prefrontal contributions to metacognition in perceptual decision making. *The Journal of Neuroscience : The Official Journal of the Society for Neuroscience*, *32*(18), 6117–6125. https://doi.org/10.1523/JNEUROSCI.6489-11.2012

Fleming, S. M., & Lau, H. C. (2014). How to measure metacognition. *Frontiers in Human*

Neuroscience, *8*, 443. https://doi.org/10.3389/fnhum.2014.00443

Fleming, S. M., van der Putten, E. J., & Daw, N. D. (2018). Neural mediators of changes of mind about perceptual decisions. *Nature Neuroscience*, *21*(4), 617–624. https://doi.org/10.1038/s41593-018-0104-6

Fleming, S. M., Weil, R. S., Nagy, Z., Dolan, R. J., & Rees, G. (2009). Relating Introspective Accuracy to Individual Differences in Brain Structure. *Science*, *324*(5928), 759–764. https://doi.org/10.1126/science.1169405

Hebart, M. N., Gorgen, K., & Haynes, J.-D. (2015). The Decoding Toolbox (TDT): a versatile software package for multivariate analyses of functional imaging data. *Frontiers in Neuroinformatics*, *8*, 88. https://doi.org/10.3389/fninf.2014.00088

Higham, P. A., Perfect, T. J., & Bruno, D. (2009). Investigating strength and frequency effects in recognition memory using type-2 signal detection theory. *Journal of Experimental Psychology: Learning, Memory, and Cognition*, *35*(1), 57–80. https://doi.org/10.1037/a0013865

Kanai, R., Walsh, V., & Tseng, C. (2010). Subjective discriminability of invisibility: A framework for distinguishing perceptual and attentional failures of awareness. *Consciousness and Cognition*, *19*(4), 1045–1057. https://doi.org/10.1016/J.CONCOG.2010.06.003

Mccurdy, L. Y., Maniscalco, B., Metcalfe, J., & De Lange, F. P. (2013). Anatomical Coupling between Distinct Metacognitive Systems for Memory and Visual Perception Decoded Neurofeedback Project for development of diagnostic and therapeutic system for mental disorders View project Temporal dynamics of visual imagery View proje. https://doi.org/10.1523/JNEUROSCI.1890-12

Meuwese, J. D. I., van Loon, A. M., Lamme, V. A. F., & Fahrenfort, J. J. (2014). The subjective

experience of object recognition: comparing metacognition for object detection and object categorization. *Attention, Perception, & Psychophysics*, *76*(4), 1057–1068. https://doi.org/10.3758/s13414-014-0643-1

Morales, J., Lau, H., & Fleming, S. M. (2018). Domain-General and Domain-Specific Patterns of Activity Supporting Metacognition in Human Prefrontal Cortex. *The Journal of Neuroscience : The Official Journal of the Society for Neuroscience*, *38*(14), 3534–3546. https://doi.org/10.1523/JNEUROSCI.2360-17.2018

Neubert, F.-X., Mars, R. B., Thomas, A. G., Sallet, J., & Rushworth, M. F. S. (2014). Comparison of Human Ventral Frontal Cortex Areas for Cognitive Control and Language with Areas in Monkey Frontal Cortex. *Neuron*, *81*(3), 700–713. https://doi.org/10.1016/J.NEURON.2013.11.012

Norman, K. A., Polyn, S. M., Detre, G. J., & Haxby, J. V. (2006). Beyond mind-reading: multi-voxel pattern analysis of fMRI data. *Trends in Cognitive Sciences*, *10*(9), 424–430. https://doi.org/10.1016/j.tics.2006.07.005

Wokke, M. E., Cleeremans, A., & Ridderinkhof, K. R. (2016). Sure I'm sure: Prefrontal oscillations support metacognitive monitoring of decision-making. *J. Neurosci*, *10*, 1612–1616. https://doi.org/10.1523/JNEUROSCI.1612-16.2016

Yokoyama, O., Miura, N., Watanabe, J., Takemoto, A., Uchida, S., Sugiura, M., … Nakamura, K. (2010). Right frontopolar cortex activity correlates with reliability of retrospective rating of confidence in short-term recognition memory performance. *Neuroscience Research*, *68*(3), 199–206. https://doi.org/10.1016/J.NEURES.2010.07.2041